The Silver Chloride Photoanode in Photoelectrochemical Water Splitting

David Schürch,[†] Antonio Currao,[†] Shaibal Sarkar,[‡] Gary Hodes,[‡] and Gion Calzaferri*,[†]

Department of Chemistry and Biochemistry, University of Bern, Freiestrasse 3, 3012 Bern, Switzerland, and Department of Materials and Interfaces, Weizmann Institute of Science, Rehovot 76100, Israel

Received: July 12, 2002

Thin silver chloride layers evolve oxygen under UV/vis illumination in aqueous solution under appropriate conditions. AgCl deposited on a conducting support photocatalyzes the oxidation of water to O_2 in the presence of a small excess of silver ions in solution. The light sensitivity in the visible part of the spectrum is due to self-sensitization caused by reduced silver species. Anodic polarization reoxidizes the reduced silver species. Considerable improvement of sensitivity has been observed with AgBr sensitized AgCl photoanodes. To test its water splitting capability, the AgCl photoanode was combined with hydrogen-producing semiconductors, such as a platinized silicon solar cell and platinized p-$GaInP_2$. AgCl layers were employed in the anodic part and the H_2 evolving semiconductors in the cathodic part of a photoelectrochemical cell for light-assisted water splitting. The AgCl electrodes were characterized with surface photovoltage spectroscopy (SPS), which identified the transition from the valence band to silver cluster levels and by in-situ UV/vis diffuse reflectance spectroscopy, which detects the reduced and reoxidized silver species.

Introduction

One of the key problems in photocatalytic water splitting is the oxidation to dioxygen, mainly because of the difficulty in accumulating the necessary four oxidative equivalents required. Different compounds have been explored as oxidation catalysts for the evolution of O_2 from water. One approach is to mimic the oxygen evolving center of photosystem II in photosynthesis.[1] Manganese complexes have been studied as models for artificial oxygen evolving centers.[2] The oxidation of water by semiconductors has been reported mainly together with H_2 producing capabilities. $InTaO_4$ doped with Ni,[3] $KTaO_3$ doped with Zr,[4] $BaTa_2O_6$,[5] and $RbNdTa_2O_7$[6] are examples where photocatalytic water splitting under irradiation was described. Investigations focusing on the photooxidation of water with semiconductors, such as WO_3[7] and Fe_2O_3,[8] can also be found in the literature. However, for all these compounds, the reported photocatalytic properties cannot be regarded as satisfactory. Their photocatalytic activity requires much improvement before any of these materials can be considered for successful applications in solar energy conversion devices.

A different approach toward water oxidation is to use silver chloride as photocatalyst. We have reported that appropriately prepared silver chloride electrodes photocatalytically oxidize water to O_2 under suitable conditions. The nanostructured silver chloride layer acts as photocatalyst in the presence of a small excess of silver cations, with a maximum evolution rate between pH 4 and 6. The photoactivity of AgCl extends from the UV into the visible light region in a process known as self-sensitization, which is due to the formation of silver species during the photoreaction.[9,10] The overall reactions involved in the photooxidation of water to O_2 are the following:

$$[n\mathrm{Ag}^+, m\mathrm{AgCl}] + \frac{r}{2}\mathrm{H_2O} \xrightarrow{\text{light}} [(n-r)\mathrm{Ag}^+, m\mathrm{AgCl}, r\mathrm{Ag}^0] + r\mathrm{H}^+ + \frac{r}{4}\mathrm{O_2} \quad (1)$$

$$[(n-r)\mathrm{Ag}^+, m\mathrm{AgCl}, r\mathrm{Ag}^0] \xrightarrow{\Delta V_{\text{Polarization}}} [n\mathrm{Ag}^+, m\mathrm{AgCl}] + r\mathrm{e}^- \quad (2)$$

In this redox reaction, water is oxidized to oxygen plus protons, and silver cations are reduced to silver upon irradiation (eq 1). Electrochemical reoxidation of the accumulated silver can be performed by anodic polarization of the electrode by means of a potentiostat (eq 2). The water oxidation reaction and the reoxidation of the reduced silver species take place simultaneously, making the system catalytic. Equation 1 has been analyzed experimentally[10] and theoretically.[11] Silver cations adsorbed at the surface of silver chloride nanocrystals are necessary for the reaction to proceed. Thus, the light absorption can be considered as a charge-transfer excitation from Cl^- to adsorbed Ag^+. The electron hole pairs may recombine, or they may separate and produce silver atoms Ag^0 and $Cl^\bullet$ radicals (eq 3). The $Cl^\bullet$ radicals recombine very fast to form Cl_2 (eq 4). The indices s and i in eq 3 and 4 refer to surface and interstitial species.

$$[m\mathrm{AgCl}]\{\mathrm{Ag}^+\}_\mathrm{s} \xrightarrow{\text{light}} [(m-1)\mathrm{AgCl}]\{\mathrm{Ag}^+, \mathrm{Ag}^0\}_{\mathrm{s,i}} + \mathrm{Cl}_\mathrm{s}^\bullet \quad (3)$$

$$2\mathrm{Cl}_\mathrm{s}^\bullet \rightarrow \mathrm{Cl_2} \quad (4)$$

Under the applied conditions ($[Ag^+] \sim 10^{-3}$ M, pH ∼ 4−6), the Cl_2 reacts with water to produce hypochlorous acid (eq 5). At lower pH and without Ag^+ excess in the electrolyte Cl_2 can be detected.[12] Silver cations act as a catalyst for the decomposition of hypochlorous acid to molecular oxygen, protons, and chloride ions (eq 6). The chloride ions are bound by the Ag^+ to form AgCl (eq 7). These reactions are very fast and it is

* To whom correspondence should be addressed. E-mail: gion.calzaferri@iac.unibe.ch.
† University of Bern.
‡ Weizmann Institute of Science.-

10.1021/jp0265081 CCC: $22.00
Published on Web 11/12/2002

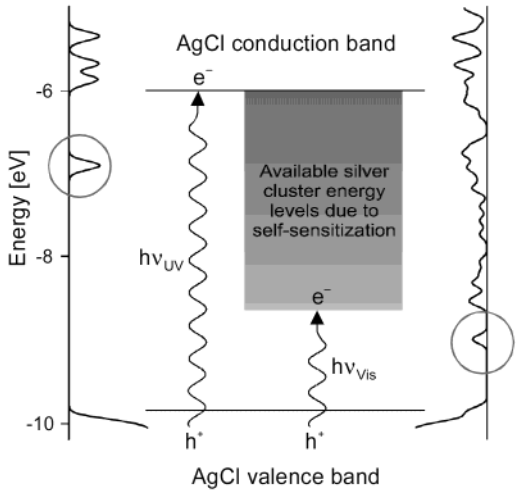

Figure 1. Proposed mechanism for the self-sensitization of AgCl with additional levels in the band gap region: (left) density of levels (DOL) for a $(AgCl)_{192}$ cluster; (right) local density of levels (l-DOL) for a $Ag_{115}/(AgCl)_{192}$ cluster composite. The lowest levels into which electrons can be excited are marked with a circle: (left) surface states (SURS); (right) metal-induced gap states (MIGS). In the center of the figure available silver cluster energy levels are shown schematiclly. For more details see refs 14 and 15.

resonable to assume that they take place at or very near the surface of the electrode.

$$Cl_2 + H_2O \rightarrow HOCl + H^+ + Cl^- \quad (5)$$

$$2HOCl \xrightarrow{Ag^+} O_2 + 2H^+ + 2Cl^- \quad (6)$$

$$[(m-1)AgCl] + Ag^+ + Cl^- \rightarrow [mAgCl] \quad (7)$$

The reduced silver atoms may react with other silver species (Ag^0 atoms, Ag^+ ions, or silver clusters) according to eq 8, forming positively charged or neutral silver clusters. In its first stages, this reaction is related to the fundamental process of latent image formation in silver halides. Continuous illumination leads to the formation of printout silver.[13]

$$Ag^0 + Ag_r^{q+} \rightarrow Ag_{(r+1)}^{q+} \qquad r \geq 1;\ 0 \leq q \leq r \quad (8)$$

The self-sensitization in the photoelectrochemical activity of AgCl is due to silver clusters adsorbed on its surface. The silver cluster/silver chloride cluster phase boundary is of particular importance for understanding all the processes involved in the AgCl electrode system. Detailed theoretical investigations on Ag/AgCl cluster composites can be found in refs 14 and 15. In the absence of silver clusters, AgCl does not absorb light below the indirect band gap transition, which is in the near UV at ~3.3 eV (~380 nm).[16] The comparison of experimental and calculated values for the ionization energy for different sized Ag clusters shows that Ag levels are located below the conduction band edge of AgCl. Additional AgCl surface states (SURS), as well as metal induced gap states (MIGS) from Ag/AgCl cluster composites are also present in the band gap region of silver chloride (see Figure 1). All these different levels are responsible for the self-sensitization of AgCl. They are available for electrons excited by light absorption below the band gap energy. The energy for all these transitions is lower than the energy needed for an optical transition from the AgCl valence band to the AgCl conduction band. Nevertheless, these new optical transitions in the visible spectral range can still initiate the oxidation of water, because the conduction band is not directly involved in the oxidation process. Thus, the photocatalytic oxidation of water on AgCl is extended from the near UV into the visible range of the spectrum. Self-sensitization as observed by us should not be confused with the spectral sensitization caused by silver clusters on silver chloride, also termed the photographic Becquerel effect. The latter observation has been attributed to electron injection from electron-donating silver clusters into the AgCl conduction band.

In this work, we present new results on AgCl as a photoanode in photoelectrochemical water splitting. The experiments were carried out using two different setups. Experimental setup 1 was used for studying the photochemical and photoelectrochemical properties of AgCl photoanodes. The influence of the layer thickness and the support roughness on the photoactivity of deposited layers will be discussed. Considerable improvement of sensitivity has been observed with AgBr sensitized AgCl photoanodes, on which we also present first results. The AgCl electrodes were characterized with surface photovoltage spectroscopy (SPS) and in-situ UV/vis diffuse reflectance spectroscopy. For testing the water splitting capability of the AgCl photoanodes, experiments were carried out in an apparatus consisting of two separate compartments connected through a salt bridge (experimental setup 2). One compartment was used for the photoanode and the other for the photocathode. A schematic representation of experimental setup 2 with respect to the electrochemical potential of the oxidation and reduction of water is shown in Figure 2. On one side, the photoanode oxidizes water to oxygen (O_2), and on the other side the photocathode reduces water to hydrogen (H_2). The electron transfer from system 1 (photoanode) to system 2 (photocathode) is achieved by polarizing the system using a potentiostat.

The AgCl photoanode was combined with semiconductors capable of reducing water to hydrogen upon illumination. Silicon has already been used in water splitting devices, in which single or multiple semiconductor p/n junctions were utilized as electrodes.[17] An early report described the use of sandwich-like semiconductor structures for the conversion of optical energy to chemical energy when immersed in an electrolyte and exposed to light.[18] This approach was used in monolithic tandem cell devices for the photoelectrochemical decomposition of water, where different semiconductor layers with different band gaps are connected in series.[19] The hydrogen producing semiconductor of this device is p-$GaInP_2$. In this work we report first photoelectrochemical water splitting experiments with AgCl as the photoanode combined with platinized silicon solar cells[20] or platinized p-$GaInP_2$[21] as the photocathode. For a detailed description of semiconductor electrochemistry and of electron transfer at electrodes and interfaces see refs 22 and 23.

Experimental Section

Experimental Setups. Two experimental setups were used for studying the photochemical and electrochemical properties of thin AgCl layers under illumination. The apparatus used in experimental setup 1 is based on a flow photoreactor system, as depicted in Figure 3. A similar apparatus had been used in experiments described elsewhere.[10,24] Its main part was a photoreactor made of poly(chlorotrifluoroethylene) (PCTFE), with an electrolyte volume of approximately 1 mL. The water and airtight inlets were used for the reference electrode and oxygen sensor, and a capillary inlet was used for the injection of air-saturated water for the calibration of the oxygen sensor. The photoreactor was connected to a nitrogen purged electrolyte reservoir (volume $\approx$ 130 mL). A peristaltic pump transported

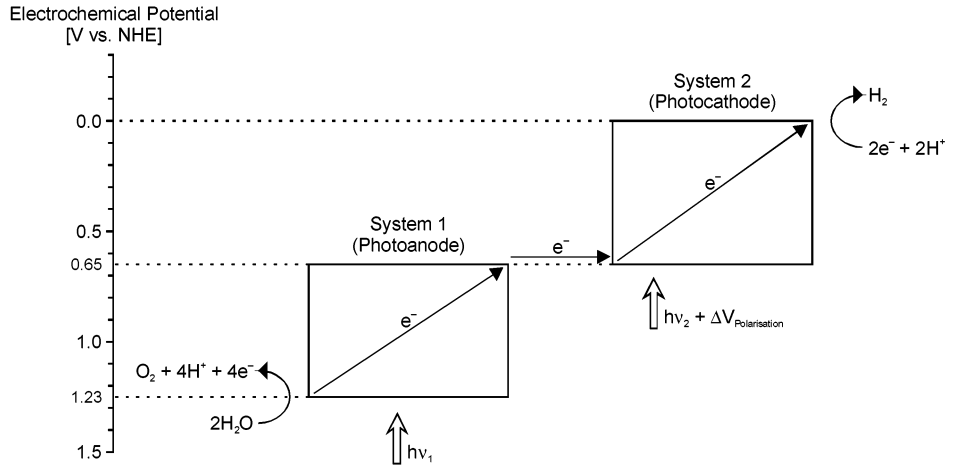

Figure 2. Schematic representation of the water splitting experiment. For the oxidation and reduction of water to O_2 and H_2, standard reduction potential values were used: $O_2 + 4H^+ + 4e^- \rightarrow 2H_2O$, $E° = 1.229$ V; $2H^+ + 4e^- \rightarrow H_2$, $E° = 0.000$ V. The electron transfer from system 1 (photoanode) to system 2 (photocathode) is achieved by polarizing with $\Delta V_{polarization}$.

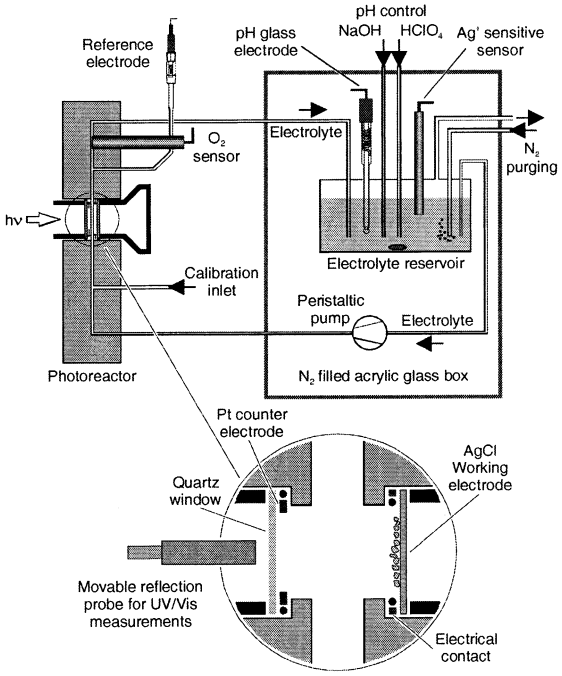

Figure 3. Experimental setup 1. Left side: photoreactor with an integrated three-electrode system, an oxygen sensor, and a capillary inlet for injection of air-saturated water for calibration of the oxygen sensor. Right side: electrolyte reservoir with N_2 purging inlet, pH glass electrode, Ag^+ sensitive sensor, and pH control inlets in a N_2-filled acrylic plastic box. A peristaltic pump transports the electrolyte from the reservoir to the photoreactor and back to the reservoir through a capillary system. Bottom: enlargement of the main part of the reactor, with quartz window, ring Pt counter electrode, and the AgCl working electrode. For UV/vis measurements a reflection probe was maneuvered in front of the window.

the electrolyte solution from the reservoir to the photoreactor and back to the reservoir, through a capillary system at a rate of about 1 mL·min^{-1}. The electrolyte reservoir, as well as the peristaltic pump, was placed in a N_2 purged acrylic plastic box. The electrolyte used in all experiments was a 0.1 M $NaNO_3$ (Merck, p.a.) aqueous solution with 1 mM $AgNO_3$ (Merck, p.a.). The pH was measured with a combined glass electrode (Metrohm, double junction, outer filling: 1 M $NaNO_3$ aqueous solution) and maintained at a value of 4.8 ± 0.5 throughout all experiments. When necessary, the pH was adjusted by adding 0.1 M $HClO_4$ (Merck, p.a.) or 0.1 M NaOH (Merck, p.a.) solution by means of dispensing units. The Ag^+ concentration was monitored by a silver ion-selective electrode (Philips, model IS 550-Ag^+). The experiments were carried out at room temperature (22 ± 1 °C). The AgCl photoanode was the working electrode in a three-electrode configuration for electrochemical experiments (chronoamperometry). The system was polarized by means of a potentiostat (Metrohm, 641 VA detector, $U_{pol} = 0.0$ V) with a platinum ring as counter electrode and a Hg/Hg_2SO_4 reference electrode (Perkin-Elmer; electrode filling, 1 M Na_2SO_4; potential, 0.64 V vs NHE). Electrically conducting SnO_2:F-coated glass supports (Siemens AG), as well as glass supports roughened by sandblasting, cut into 20 mm diameter disks were used as electrode supports (for electrode preparation, see section below). The Pt counter electrode in the photoreactor was protected from illumination by a black plastic ring with an inner diameter of 9 mm; the illuminated area of the working electrode was thus 0.64 cm^2. A 450 W xenon arc lamp (Osram, XBO 450 W OFR) mounted in a lamp housing (PTI, A6000) in conjunction with a power supply (PTI, LPS 1100) was used as the light source. The light was passed through a stainless steel IR filter, filled with distilled water as absorption liquid, then collimated with lenses, and passed through a light filter (Schott, KG3; 50% transmission range, 330−700 nm), before illuminating the AgCl electrode with an incident intensity of about 100 mW·cm^{-2}, measured with a radiant power/energy meter (Oriel Instruments, model 70260). In the experiments described, the AgCl electrode was exposed to successive illumination and dark periods of 100 and 25 min duration each. The experimental setup was interfaced to a computer via a GPIB bus and a QBasic program was implemented for data collection and control of various components.

Experimental setup 2 consisted of two separate compartments connected through a salt bridge (see Figure 4). One compartment was used for the AgCl photoanode, and the other for the photocathode (see below for more details). The apparatus was made of acrylic plastic (PMMA, poly(methyl methacrylate)). Both cell compartments had different water and airtight inlets for the pH glass electrode, argon gas (inlet and outlet), pH control dispensing unit, reference electrode, and O_2 or H_2 sensor, respectively. A holding device was used for mounting and contacting the electrode in each cell. For the salt bridge a jelly like electrolyte was used. A hot solution of 1.7 g of Agar (Fluka) in 100 mL of 0.1 M KNO_3 (Merck, p.a.) aqueous solution was poured into the bridge and left to solidify by cooling overnight.

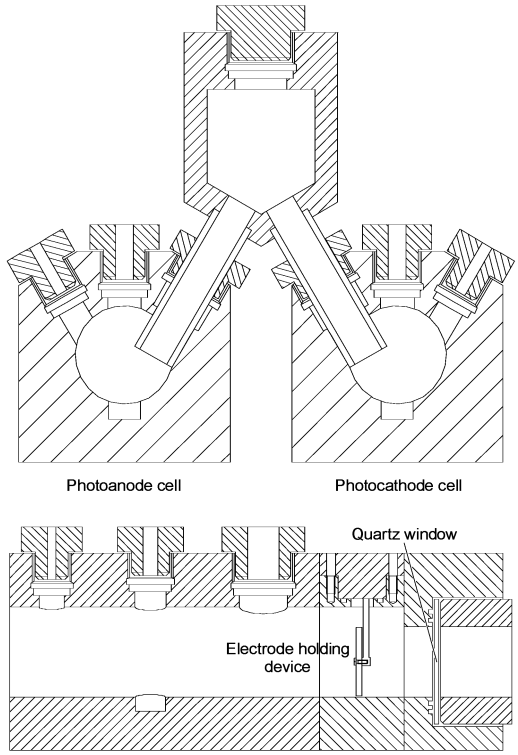

Figure 4. Experimental setup 2. Top: front view cross section of both cells and salt bridge. Bottom: side view cross section of a cell with holding device for the electrode. The water and airtight inlets were used for the pH glass electrode, argon inlet and outlet, pH control dispensing unit, reference electrode, and O_2 or H_2 sensor, respectively.

The electrolyte volume in both cells was approximately 75 mL. Before data acquisition began, the electrolyte was thoroughly purged with argon. Both cell compartments were under argon atmosphere throughout all experiments. For the AgCl photoanode cell, a 0.1 M KNO_3 aqueous solution with 1 mM $AgNO_3$ was used. The electrolyte for the photocathode cell was a 0.1 M KNO_3 aqueous solution. Each cell compartment was magnetically stirred. In both cell compartments the pH was measured with a combination pH glass electrode (Thermo Orion; Ross pH electrode; internal filling solution, 1 M KNO_3), and maintained at 4.5 ± 0.5 for the photoanode and at 1.5 ± 0.3 for the photocathode cell. One dispensing unit for each cell compartment was used for adjusting the pH, if necessary, with 0.1 M KOH (Merck, p.a.) or 0.1 M HCl (Merck, p.a.) solution, respectively. The experiments were carried out at room temperature (22 ± 1 °C). In all electrochemical experiments the AgCl photoanode was the working electrode in a three-electrode system. Polarization was applied by a potentiostat (Metrohm, 641 VA detector, $U_{pol} = 0.0$ V) with a Hg/Hg_2SO_4 reference electrode (Perkin-Elmer; electrode filling, saturated K_2SO_4 aqueous solution; potential, 0.65 V vs NHE) in the photoanode compartment and platinum, silicon solar cell, or p-$GaInP_2$ as the counter electrode (see below for more details). The second Hg/Hg_2SO_4 reference electrode in the setup was used for measuring the potential at the back contact of the photocathode. A 1000 W xenon arc lamp was used as the light source (Osram, XBO 1000 W/HS OFR), with a power supply (LPS 1000) and lamp housing (A5000) from PTI. To reject the IR part of the lamp radiation, a stainless steel IR filter filled with distilled water as the absorption liquid was placed on top of the lamp housing. The light beam was collimated with lenses and passed through a light filter (Schott, KG3; 50% transmission range, 330−700 nm), before it was split with a beam splitter (polka dot beam splitter, Oriel Instruments), illuminating both cell compartments simultaneously. The incident light intensity at the location of the AgCl electrode was about 100 $mW \cdot cm^{-2}$, measured with a radiant power/energy meter (Oriel Instruments, model 70260). In all experiments described for setup 2, both cell compartments were exposed to successive illumination and dark periods of 90 and 45 min duration each. If only the photoanode cell was to be illuminated, a black cardboard cover was placed in front of the photocathode cell. All the various components of the experimental setup were connected to a multimeter (Keithley, model 2000 with scanner card) that was controlled by a computer via a GPIB bus. Data acquisition was monitored and stored on file by a program written in QBasic. For all figures, the measured potentials were converted to values versus a normal hydrogen electrode (NHE).

Oxygen and Hydrogen Detection. Determination of the oxygen and hydrogen concentrations were carried out in situ by electrochemical measurement with sensors (WTW, model EO 96). For the oxygen detection an unmodified sensor was connected to a potentiostat (Metrohm, 641 VA detector). The polarization potential of the gold cathode of the sensor was −0.75 V vs an internal Ag/AgCl reference electrode, which also served as the counter electrode. The sensor cap fitted with a gas permeable membrane was filled with an electrolyte made of an aqueous solution of 0.75 M KCl (Merck, p.a.) and 0.25 M NaOH. For hydrogen detection the tip of the gold electrode of the sensor was electrochemically platinized in a 2% H_2PtCl_6 (Fluka, p.a) aqueous solution. The platinization was done potentiostatically, using a platinum wire as the counter and reference electrodes. A voltage of −1.5 V was applied for about 5 min. The applied polarization potential for the H_2 sensor was 0.40 V vs an internal Ag/Ag_2SO_4 reference electrode, which also served as the counter electrode. The sensor cap was filled with a 0.1 M H_2SO_4 aqueous solution saturated with Ag_2SO_4 (Fluka, p.a.). The O_2 sensor was calibrated by injecting air-saturated water into the cell (temperature, 25 °C; O_2 concentration at 1 atm air pressure, 0.267 mM or 8.55 $mg \cdot L^{-1}$).[25] For the calibration of the H_2 sensor the anodic current signal, i.e., the charge transferred from the photoanode to the photocathode cell in setup 2, was used to calculate the H_2 production. The H_2 sensor signal was scaled accordingly. During the dark periods of an experiment, the O_2 and H_2 sensor signals decreased in all results presented, because both setups were under constant inert gas purging.

Preparation of AgCl-Coated Electrodes as Photoanode. Two types of AgCl electrode preparation procedures were used. Precipitated layers were only prepared for surface photovoltage spectroscopy (SPS) measurements (see section below for more details). The second type of electrodes were used for photoelectrochemical experiments with setups 1 and 2. The AgCl layers were prepared by electrochemical oxidation of Ag layers on different supports with a conducting Au layer. The notation used for distinguishing between electrodes in the Results and Discussion gives the thickness of the deposited Au and Ag layers in brackets. After oxidation of the Ag layers, the color of the electrochemically produced AgCl electrodes was light-gray to gray for both supports, indicating a small amount of reduced silver. The morphology of AgCl layers was investigated by scanning electron microscopy (SEM) carried out with a JEOL microscope (JSM-840).

Precipitated AgCl Layers. Electrically conducting SnO_2:F-coated glass was used as electrode support (Siemens AG, conducting layer: $\sim 1\ \mu m$). The 1 mm thick glass support was cut into 20 mm diameter disks. Before coating, they were

SCHEME 1: AgCl Layers on Different Glass Supports

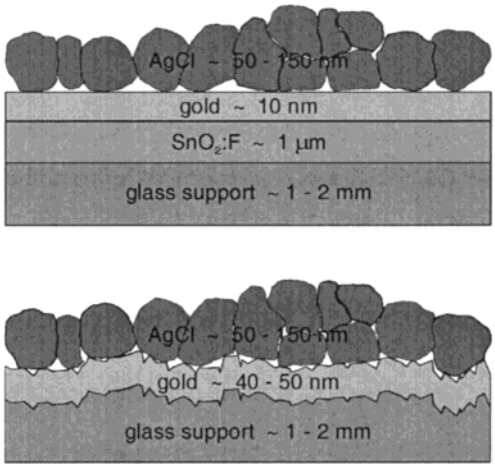

cleaned in aqua regia, polished with an aqueous suspension of Al_2O_3 (Presi, 0.3 μm Al_2O_3), washed ultrasonically in ethanol, and dried. The glass support was placed in a small beaker (23 mm diameter) and covered with 2 mL of bidistilled water. First, 20 μL of 0.1 M $AgNO_3$ (Merck, p.a.) aqueous solution was added, followed by 20 μL of 0.1 M NaCl (Merck, p.a.) solution. After mixing, sedimentation of AgCl was allowed in the dark overnight. The white AgCl-coated electrode was dried at room temperature. About 3.5 mm of the outer edge of the sedimented layer was wiped away for the electrical contact. The amount of AgCl on the remaining area was estimated to be 65 μg, or 0.46 μmol, corresponding to an equivalent charge of 44 mC on an electrode area of about 1.3 cm^2.

AgCl Electrodes for Experimental Setup 1. Scheme 1 represents AgCl layers on different supports. The standard glass supports had a conducting SnO_2:F layer; the ones with a rough surface were sandblasted with glass powder particles (0.25−0.5 mm diameter). For experimental setup 1 both kinds of support were used. The 20 mm diameter disks had a predeposited gold layer. The only exception was SnO_2:F-coated glass supports used for surface photovoltage spectroscopy (SPS, see section below) where no Au layer was deposited. For AgCl electrodes on SnO_2:F-coated glass, the Au layer was 10 nm; for supports roughened by sandblasting, it was 40 nm thick. For the silver deposition, a cover ring was placed on the support, covering 3.5 mm of the outer edge, which would be used for back contacting the AgCl anode. On the central part of the support, a 50 or 100 nm Ag layer was deposited (12 mm diameter). Depositions of gold and silver layers were carried out by physical vapor deposition (PVD) in a high vacuum coating system (Bal-Tec, MED 020). The silver layer was electrochemically oxidized in 0.2 M KCl (Merck, p.a.) aqueous solution at pH 2, adjusted with 25% HCl (Hänseler AG, p.a.). For the Br-doped AgCl layers, a small amount of NaBr (Merck, p.a.) was added to the KCl solution. Layers were prepared for different Br concentrations in the electrolyte (0.05−0.20 mM). A three-electrode setup was used, where the coated glass support was the working electrode, a platinum wire was the counter electrode, and a Ag/AgCl was the reference electrode. With a computer-controlled potentiostat (EG&G, model 273A), an anodic potential sweep from 0.0 to 0.9 V was performed at a rate of 100 mV·s^{-1}. The potential sweep showed an oxidation peak at about 0.4 V with a maximum current density of ~14 mA·cm^{-2}. The charge transferred was approximately 80 mC for a 50 nm and 170 mC for a 100 nm Ag layer, respectively, calculated from the integrated current peak. Thus, the amount of AgCl produced was 0.83 μmol (118.8 μg) or 1.76 μmol (252.5 μg), respectively, for an electrode area of about 1.3 cm^2.

AgCl Electrodes for Experimental Setup 2. The round glass support (~2 mm thick) had a diameter of 24.5 mm. Two small grooves at the edge were used for mounting the support on the sample holder with poly(ethylene terephthalate) (PET) screws. Only AgCl layers on glass supports roughened by sandblasting were prepared for setup 2. Before coating, the glass support was washed ultrasonically in ethanol and dried. A 50 nm gold layer was first deposited. Next, a 150 nm Ag layer was deposited on almost the whole Au covered support, except for a 1.5 mm wide rim at the edge of the grooves covered by pins. The Au rim was necessary for contacting the support to the holding device. The electrochemical oxidation of the Ag layer to AgCl was carried out as described above. The potential sweep showed an oxidation peak at about 0.4 V with a maximum current density of ~7 mA·cm^{-2}. The charge transferred was approximately 1.2 C. Thus, the amount of AgCl produced was 12.4 μmol (1.78 mg), for an AgCl covered electrode area of approximately 4.5 cm^2.

Preparation of Cathodes. For the photocathode cell of experimental setup 2, platinum, silicon solar cells,[20] and p-$GaInP_2$[21] were used as electrodes. For the platinum counter electrode, a 50 nm Pt layer deposited by PVD on a conducting glass support, as well as a Pt foil (0.1 mm thick, Johnson Matthey) were used. Silicon solar cells were cut into square pieces of 17 × 17 mm^2. The top and rear contact fingers of the solar cell were removed by the following treatment. First, the cell was dipped into a 30% H_2O_2/95% H_2SO_4 solution (volume ratio 1:1) for about 24 h. Afterward, aqua regia was used for a further 24 h. This procedure was repeated if residues were still present after the treatment. The solar cell was then etched in a 20−25% HF solution and platinized in a 1.5% H_2PtCl_6 (Fluka, p.a) aqueous solution. The platinization was carried out potentiostatically, using a platinum wire as the counter and reference electrodes. A voltage of −2 V was applied for about 20 min. Only the n-side of the solar cell was platinized, whereas the p-side was covered with adhesive tape. As back contact for the platinized solar cell, a conducting SnO_2:F-coated glass support with a 50 nm Au layer was used. The platinized solar cell was pressed and fixed on the support with a small amount of epoxy adhesive at the edges of the cell.

The p-$GaInP_2$ was supplied as a wafer with a copper wire attached to the back as contact. It was surrounded by a glass tube (diameter 6 mm) and insulated from the electrolyte by an epoxy coating that also covered the sample edges, exposing only an approximately 3 × 4 mm^2 sample area (see ref 21 for more details). To reduce the overvoltage, a thin layer of platinum catalyst was electrochemically deposited on the surface of the electrode according to the procedure described above.

Surface Photovoltage Spectroscopy (SPS). This technique is based on the classic Kelvin probe.[26] In SPS the difference in surface work functions between materials known as the contact potential difference, CPD, is measured as a function of incident photon energy. The sample to be measured and a metal reference are placed in a capacitor arrangement, with the distance between them kept to a fraction of a millimeter. When the metallic reference is vibrated the resulting ac capacitance gives rise to an ac current in the external circuit which is nullified by an opposing dc bias, equal and opposite to the CPD between sample and reference. Illuminating the sample generates free charge carriers (i.e., holes and electrons). Light absorption leads to a charge redistribution within the sample, and hence a change in the CPD can be observed. This way band gap and sub-bandgap

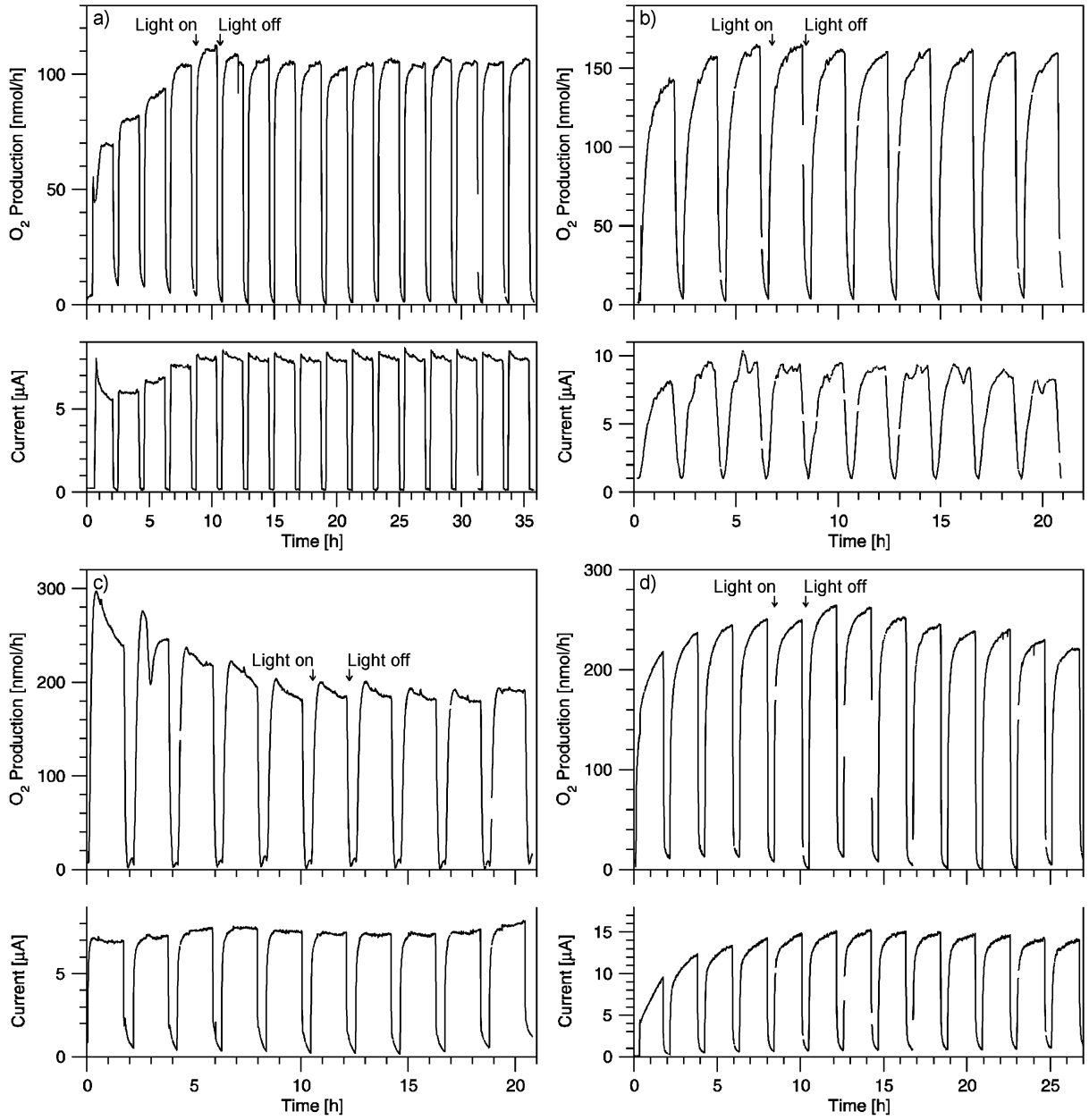

Figure 5. Oxygen production and anodic photocurrent vs time for AgCl electrode experiments carried out with experimental setup 1 with illumination and dark periods: (a) AgCl layer on a SnO_2:F-coated glass support (deposited layers: Au, 10 nm; Ag, 50 nm); (b) AgCl layer on a SnO_2:F-coated glass support (deposited layers: Au, 10 nm; Ag, 100 nm); (c) AgCl layer on a roughened glass support (deposited layers: Au, 40 nm; Ag, 100 nm); (d) AgCl layer on a SnO_2:F-coated glass support with small amounts of AgBr incorporated in the layer (deposited layers: Au, 10 nm; Ag, 100 nm).

(i.e., surface state) transitions can be detected. SPS was carried out on precipitated and electrochemically prepared AgCl layers at room temperature and under ambient conditions. The layers were prepared on a SnO_2:F-coated glass support without an intermediate Au layer (deposited layer for electrochemically prepared AgCl: Ag: 50 nm), with the exception for the measurement of a AgCl electrode after a 24 h experiment where a 10 nm Au layer was first deposited. A commercial Kelvin probe unit (Besocke Delta PHI GmbH, Germany) with a sensitivity of ~1 mV was used for the measurements. The sample surface was illuminated by light from a 600 W tungsten−halogen lamp passing through a 0.5 m grating monochromator (Spex 270M).

UV/Vis Measurements. With experimental setup 1, in situ diffuse reflectance measurements of the AgCl photoanode were taken during the course of an experiment. Spectra were taken with a deep well spectrometer (Ocean Optics, S1024DW) equipped with a reflection probe with one reading and six illuminating optical fibers and a deuterium/halogen light source (Top Sensor Systems, i.e., Avantes, DH-2000-FHS). The reflection probe was integrated into an *xy* directional telescopic arm, which could be quickly brought into measuring position and back again by stepping motors.

Linear Potential Sweep Experiments. For investigating the influence of illumination on the silicon solar cell photocathodes, linear potential sweep experiments were carried out with experimental setup 2. Platinized and nonplatinized silicon solar cells, as well as a 50 nm Pt layer deposited by PVD on a conducting glass support were used in the photocathode cell. By means of a buffer operational amplifier (opamp), the potential difference between a AgCl photoanode and a Hg/Hg_2SO_4 reference electrode (Perkin-Elmer; electrode filling, saturated K_2SO_4 aqueous solution; potential, 0.65 V vs NHE) was kept at ~0 V, corresponding to the applied polarization

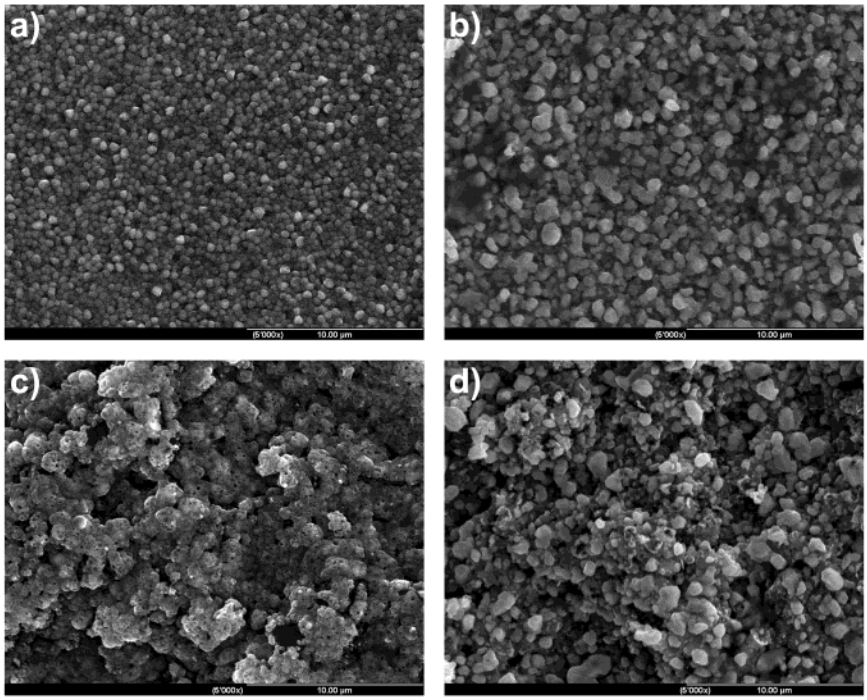

Figure 6. SEM images of AgCl electrode surfaces (5000× magnification) before and after an experiment. (a) and (b) show a AgCl layer on a SnO_2:F-coated glass support, (c) and (d) show a AgCl layer on a roughened glass support (deposited layers: Au, 10 and 40 nm, respectively; Ag, 100 nm).

potential during a standard experiment. The AgCl electrode was connected to the buffer output, the reference electrode to the noninverting input, and the photocathode to the supply ground of the buffer opamp. Linear potential sweeps were performed with a computer-controlled potentiostat (EG&G, model 273A) where the current was monitored as a function of the applied potential. In a three-electrode setup the photocathode was the working electrode and the AgCl photoanode the counter electrode, together with a Hg/Hg_2SO_4 reference electrode. Measurements were carried out by illuminating both the photoanode and photocathode cell, as well as only the photoanode cell.

Results and Discussion

Photocatalytic Oxidation of Water to O_2. Experimental setup 1 was used for photocatalytic water oxidation experiments. In Figure 5 the results from different AgCl electrodes can be compared. We previously showed that a significant improvement in photocatalytic oxidation of water to O_2 was realized when the AgCl layers were deposited on gold rather than directly on a conducting SnO_2:F-coated glass support.[9] In particular, layers on gold showed a much improved stability in the O_2 and current signals with no noticeable decrease even after several hours of reaction. This is probably due to the improved mechanical stability and the contact between the Ag species formed during an experiment and the gold substrate, which allows a better reoxidation, particularly during the first few cycles.[27] Figure 5a shows the results of a typical experiment with setup 1. An AgCl layer on gold-modified SnO_2:F-coated glass support showed a sustained O_2 production around 100 nmol·h^{-1} (deposited layers: Au, 10 nm; Ag, 50 nm). The notation used for distinguishing between electrodes gives the thickness of the deposited Au and Ag layers in brackets.

One of the main problems affecting the quantum efficiency of the Ag/AgCl system is the low light absorption by the layer. One approach is to increase the layer thickness, and/or the surface area, and thus the amount of light absorbed. The improved contact afforded by the gold substrate gave the impetus to try experiments with thicker layers, the idea being to increase the layer's absorptivity and with the improved contact, hopefully still get an efficient reoxidation. For a thicker AgCl layer, one simply has to increase the amount of Ag deposited on the support. The results of a typical experiment with such a layer are shown in Figure 5b (deposited layers: Au, 10 nm; Ag, 100 nm). The O_2 production level sustained at around 160 nmol·h^{-1} is significantly higher than that achieved with the thinner layers. The improvement is certainly due to the greater amount of AgCl present, which increases layer absorptivity and therefore the product yield. Twice the amount of Ag leads to about 1.6 times more O_2. The photocurrent is also somewhat higher although proportionately less than the O_2 production rate.

A different approach for increasing the low absorptivity of AgCl layers is to change the surface morphology of the AgCl layers. The results of an experiment with a sandblasted glass support are shown in Figure 5c (deposited layers: Au, 40 nm; Ag, 100 nm). After a slight decrease during the first part of the experiment, a steady and increased O_2 production at around 200 nmol·h^{-1} can be observed, compared with the results in Figure 5b. The roughening of the surface of the support by sandblasting is also responsible for a change in surface morphology of the AgCl layers. Figure 6 shows SEM images of AgCl layers before and after an experiment, on SnO_2:F-coated and on roughened glass supports. The two types of electrodes are strikingly different in their morphology. Before illumination, the layer on SnO_2:F-coated glass appears quite homogeneous and flat with well-defined particles between 300 and 800 nm in diameter. In contrast, the layer on the sandblasted glass is porous, very rough, and riddled with holes. After illumination, the layer on the SnO_2:F-coated glass is somewhat rougher and less homogeneous with a greater range in particle size from about 200 to 1000 nm. That on the sandblasted support retained the spongelike

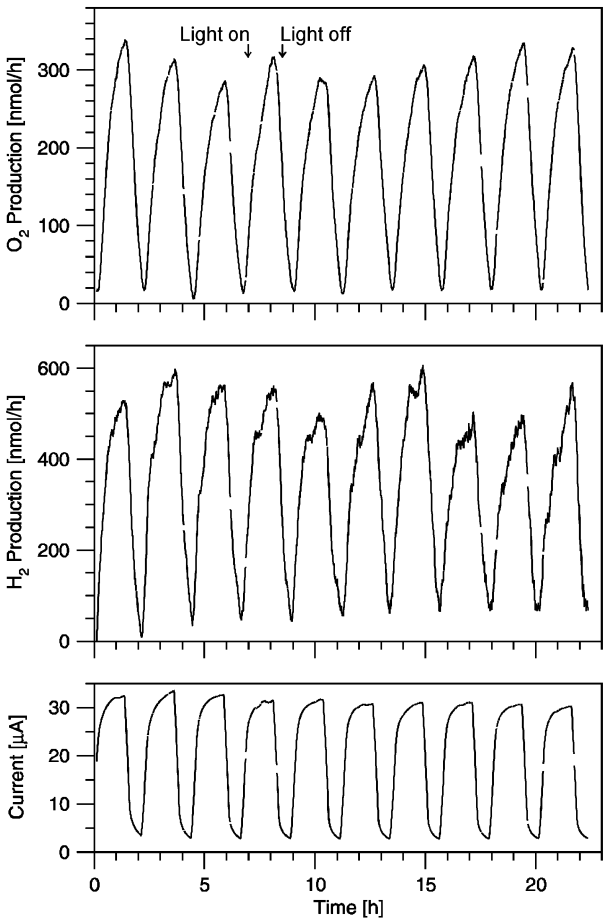

Figure 7. Oxygen and hydrogen production and anodic photocurrent vs time for a AgCl layer on a roughened glass support combined with a 50 nm Pt layer on a SnO_2:F-coated glass support, carried out with experimental setup 2 (deposited layers: Au, 50 nm; Ag, 150 nm).

morphology, only now with better defined particles. Here too, the layer is less homogeneous with particles ranging from 200 to 1000 nm in diameter.

To increase the absorptivity of the AgCl photoanodes, the addition of sensitizing agents, chemical species which have a high absorptivity in the visible light spectrum, was tested. This approach is effectively used to greatly increase the light sensitivity of silver halide photographic films and it is likely that the sensitivity of our layers can also be improved in this manner. A number of experiments were carried out with small amounts of Br^- incorporated into the AgCl layer. The layers were made electrochemically in the usual fashion, but with the addition of small amounts of NaBr to the KCl electrolyte used for the electrochemical oxidation of the Ag layer. Best results were obtained from layers made with a Br^- concentration of 0.05 mM in the electrolyte, an example of which is shown Figure 5d. The results show the sensitization approach to be a promising one, with an O_2 production level peaking at 260 nmol·h^{-1} and slightly decreasing afterward.

Photoelectrochemical Water Splitting. Experimental setup 2 was used for water splitting capability tests of AgCl photoanodes when combined with hydrogen producing (photo)cathodes. For the AgCl layer, only glass supports roughened by sandblasting were used. The two separate compartments of the setup were connected through a salt bridge. One was used for the photoanode and the other for the counter electrode or photocathode. In Figure 7 the results of a typical experiment using a AgCl photoanode combined with a platinum electrode are shown. No significant difference was observed in photocatalytic experiments whether Pt on a SnO_2:F-coated glass support or a Pt foil was used as the counter electrode. Sustained oxygen and hydrogen production can be observed. The amount of oxygen formed is comparable to that observed using experimental setup 1, if the greater AgCl electrode area is taken into account.

The AgCl photoanode was also combined with semiconductors capable of reducing water to hydrogen upon illumination. In Figure 8a the results of one experiment with a platinized silicon solar cell as photocathode are shown. Oxygen and hydrogen production can be observed, making the overall water splitting photoassisted. The silicon solar cell was illuminated from the n-doped side. A schematic drawing of the approximate position of the band edges under illumination is shown in Figure 9. The potential measured at the back contact decreased due to the photovoltaic effect of the solar cell. As expected for commercially available solar cells, the potential decreased approximately 0.4 V. This potential change was monitored throughout an experiment.

Water splitting capability tests were also carried out with platinized p-$GaInP_2$ as photocathode. Figure 8b shows the results of a typical experiment, and in Figure 10 the approximate positions of the band edges of p-$GaInP_2$ are schematically drawn. The values for the band edge positions were taken from ref 21. These values shift with the carrier concentration and the surface morphology of the semiconductor, as well as the pH of the electrolyte. Therefore, they should be regarded as only approximate. For both photocathode materials, i.e., silicon and p-$GaInP_2$, the potential measured under illumination at the back contact was used to determine the position of the Fermi level in Figures 9 and 10. In a 0.1 M KNO_3 aqueous solution at pH ~1.5, the values are ~0.4 and ~0.5 V vs NHE, for silicon and p-$GaInP_2$, respectively. The AgCl photoanode is polarized at 0.65 V vs NHE. Therefore, for both semiconductors, the position of the Fermi level under illumination is approximately 0.25 and 0.15 V, too small to allow the system to work without polarization. Despite the fact that the AgCl photoanode still has to be polarized, the combination with silicon solar cells or p-$GaInP_2$ as photocathode makes the overall water splitting photoassisted.

Linear Potential Sweep Experiments. Platinized and nonplatinized silicon solar cells, as well as a 50 nm Pt layer deposited by PVD on a conducting glass support, were used in the photocathode cell of experimental setup 2 for linear potential sweep experiments. Figure 11 shows that by illuminating the AgCl photoanode as well as the silicon photocathode (nonplatinized, dash, a_1; platinized, dash−dot, b_1), the potential required, compared to that needed if only the AgCl photoanode is illuminated (nonplatinized, dash, a_2; platinized, dash−dot, b_2), is decreased. For comparison, the corresponding curves for platinum as counter electrode are included in the figure (solid, c_1 and c_2), where the illumination does not much affect the linear potential sweep. For example, if both electrodes are illuminated, a cathodic current starts to flow from the AgCl photoanode to the platinized silicon solar cell at an applied potential of ~0.45 V vs NHE. This value is in agreement with the potential measured at the back contact and used to determine the position of the Fermi level for platinized silicon in Figure 9. If only the AgCl electrode is illuminated, the cathodic current starts at a more negative potential, ~0.1 V vs NHE. The polarization potential applied to the AgCl electrode is 0.65 V vs NHE. This is only 0.20 V more positive than the onset potential measured during the potential sweep when both cells are illuminated.

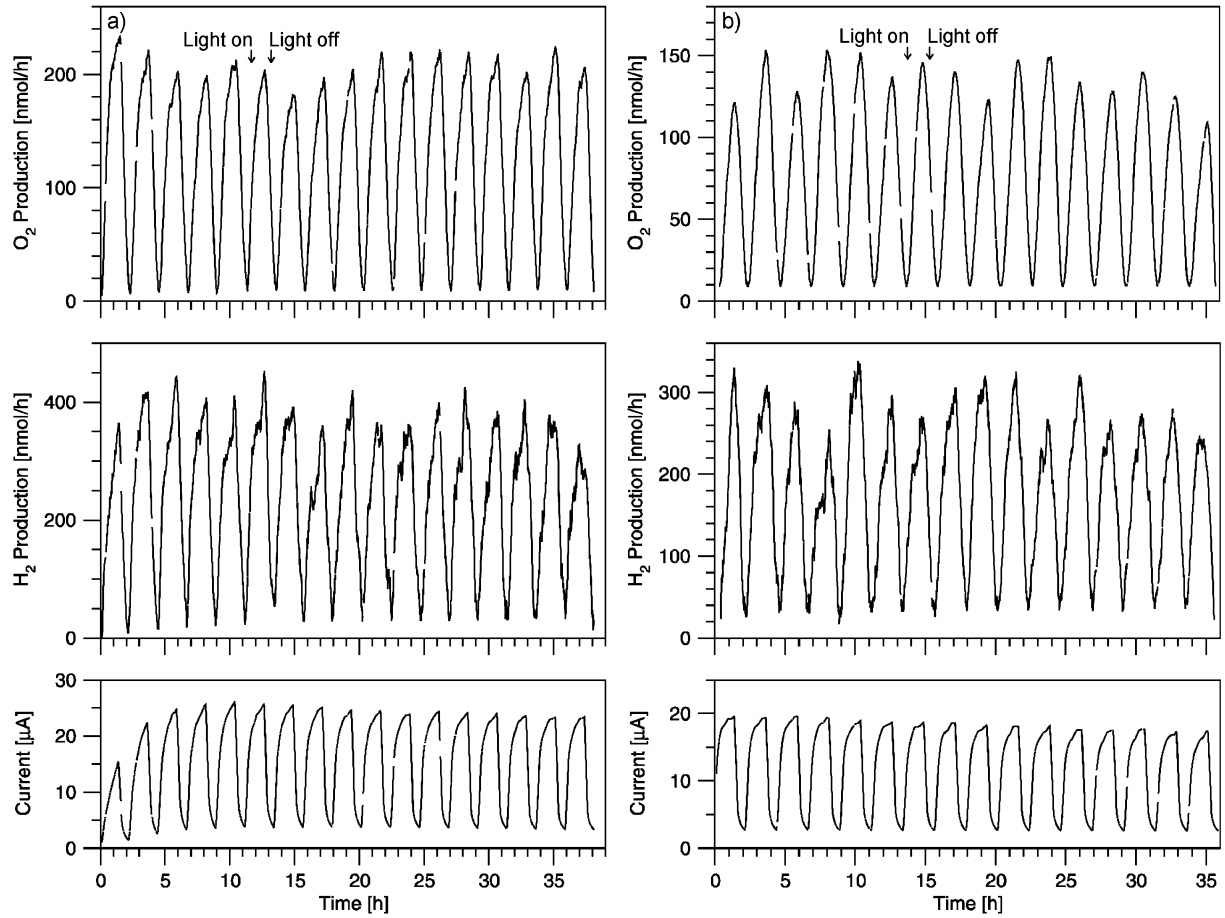

Figure 8. Oxygen and hydrogen production and anodic photocurrent vs time for AgCl layers on a roughened glass support (deposited layers: Au, 50 nm; Ag, 150 nm) combined with different photocathodes, carried out with experimental setup 2 with illumination and dark periods: (a) AgCl electrode combined with platinized silicon solar cell; (b) AgCl electrode combined with platinized p-$GaInP_2$.

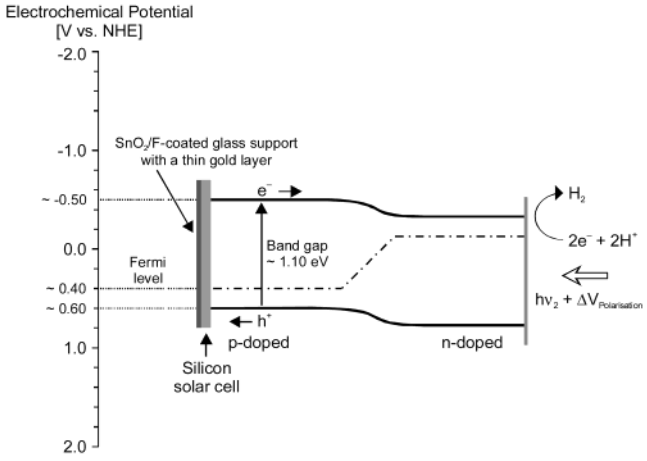

Figure 9. Band gap scheme for a silicon solar cell as photocathode under illumination from the n-doped side.

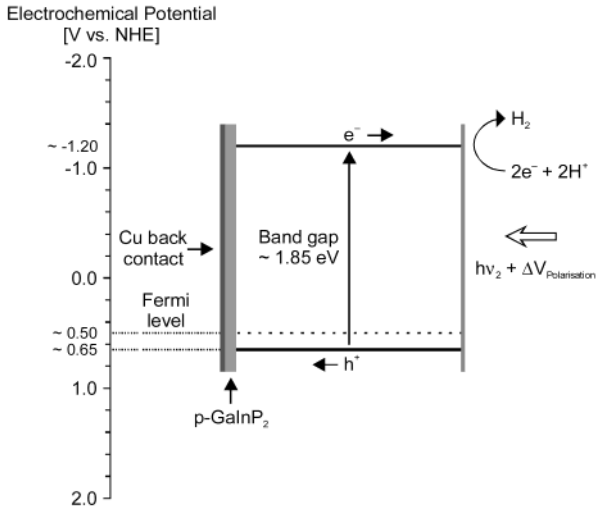

Figure 10. Band gap scheme for p-$GaInP_2$ as photocathode under illumination.

Surface Photovoltage Spectroscopy. Surface photovoltage spectroscopy (SPS) measurements were carried out on AgCl layers. This technique provides valuable information about the electronic structure of the various layers. SPS analysis was carried out on two different types of AgCl layers, one produced electrochemically and the other by sedimentation for comparison. Figure 12a shows an onset of the contact potential difference (CPD) signal at ~700 nm and a second transition at ~400 nm for an electrochemically prepared AgCl layer. The onset at ~700 nm is attributed to valence band to surface state transitions, more specifically from the AgCl valence band to empty silver states. This interpretation is consistent with the "p-type" response (positive CPD on illumination): This means that the silver states extend ~1.4 eV below the conduction band of AgCl, which is in good agreement with values we have previously calculated.[11,14,15] It should be noted that this spectroscopically visible silver was not produced by layer illumination but instead is the result of an incomplete silver oxidation to AgCl during the electrochemical synthesis. The second signal onset at ~400 nm, also p-type response, is clearly the valence

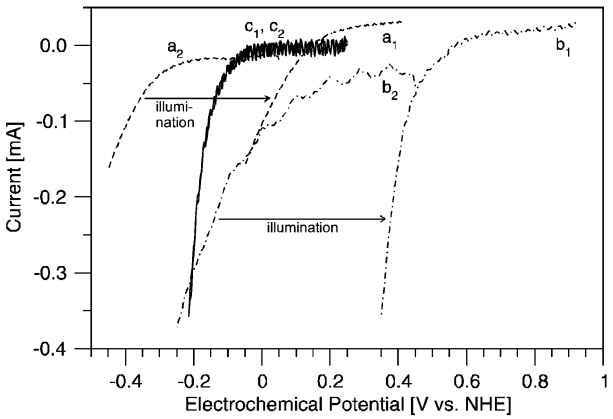

Figure 11. Linear potential sweep experiments carried out with experimental setup 2. Platinized and nonplatinized silicon solar cells and a 50 nm Pt layer deposited by PVD on a conducting glass support were used in the photocathode cell. Cathodic current has a negative sign and is drawn downward, and the potential is shown vs NHE (normal hydrogen electrode). Illuminated photocathode cell: nonplatinized silicon solar cell (dash, a_1), platinized silicon solar cell (dash−dot, b_1), platinum (solid, c_1). Dark photocathode cell: nonplatinized silicon solar cell (dash, a_2), platinized silicon solar cell (dash−dot, b_2), platinum (solid, c_2).

band to conduction band transition and is in good agreement with the reported indirect band gap of AgCl.[28] The sedimented layer in Figure 12b shows signal onsets at ∼600 and ∼400 nm. The onset at ∼600 nm is again presumed to be due to valence band Ag surface state transitions. Here the Ag states extend ∼1.1 eV below the conduction band, significantly less than in the case of electrochemically prepared layers. It is possible that silver cluster species are responsible for the shorter wavelength signal onset because the accessible levels are higher energy than those of larger silver aggregates or bulk silver (see Figure 1). This conclusion is consistent with the fact that in the case of the sedimented layers, there was no bulk silver present immediately after sedimentation: the layers were white. The silver species that did form (slight coloration visible to the eye) were due to coincidental light exposure, which was not enough to form bulk silver. The photovoltage is considerably higher than for the electrochemically prepared AgCl. This could be due to greater band bending in the more stoichiometric sedimented layer. Another possible reason is that the electrochemically prepared sample is likely to be more highly doped than the whiter and probably more stoichiometric sedimented one. This implies a narrower space charge layer. If the space charge layer is too narrow, then the SPS signal will be low.

An SPS spectrum for an electrochemically prepared AgCl electrode on gold after a 24 h experiment in the flow photoreactor (setup 1) is shown in Figure 12c. There is a clear onset of the CPD signal at ∼600 nm, in the opposite direction (i.e., n-type response) to the previous spectra and considerably weaker. The n-type response could be due to the depopulation of surface states, i.e., transitions from surface states to the AgCl conduction band or to states near the conduction band. This would explain the weak signal as transitions from surface states are normally very weak.

UV/Vis Measurements. In situ characterization of the AgCl electrode was carried out with UV/vis diffuse reflectance spectroscopy. The reduced and reoxidized silver species are spectroscopically visible. Spectra were taken in situ during the course of a typical AgCl electrode experiment with experimental setup 1. Figure 13 shows the oxygen production and the photocurrent for several light and dark cycles. The corresponding

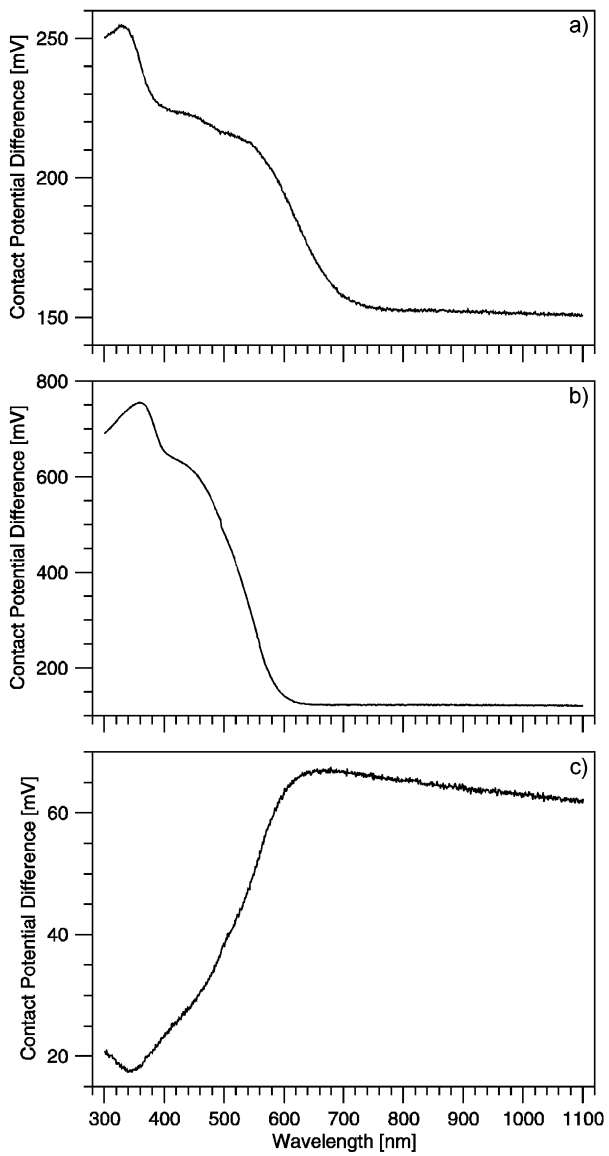

Figure 12. Surface photovoltage spectra of AgCl layers on a SnO_2:F-coated glass support: (a) electrochemically prepared AgCl layer before experiment (deposited layer: Ag, 50 nm); (b) sedimented AgCl layer before experiment; (c) electrochemically prepared AgCl layer after a 24 h experiment (deposited layers: Au, 10 nm; Ag, 50 nm).

spectra shown in Figure 14 were taken at the indicated times during the course of the experiment.

The spectra show no distinct features, which is expected because new electrochemically prepared AgCl electrodes are gray or brown and thus absorb (or reflect) similarly over a broad range of the visible spectrum. The sharp peak at ∼660 nm is not characteristic of AgCl but a remnant of the deuterium/halogen light source. The large decrease in reflectance over the entire visible region within the first 2 min is due to the formation of silver species on or near the AgCl surface, which causes a visible darkening of the layer, an effect well-known in silver halide photography.[13] As the photoreaction proceeds, fresh AgCl and Ag are formed at the electrode surface, resulting in an entirely new morphology that is more reflective than the original layer (see SEM images in Figure 6). This development is represented by the steadily increasing reflectance up to the fourth cycle, after which time the reflectance stays almost constant, as shown in the spectrum taken during the start of cycle 12. X-ray fluorescence measurements have shown that the degree of reflectance increase is correlated with the amount of silver

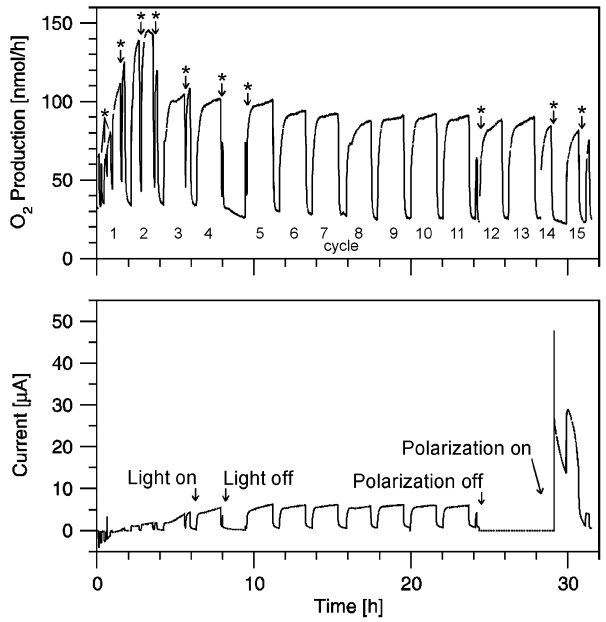

Figure 13. Oxygen production and anodic photocurrent vs time for a AgCl layer on a SnO_2:F-coated glass support carried out with experimental setup 1, with illumination and dark periods (deposited layers: Au, 10 nm; Ag, 50 nm). The cycle numbers correspond to the numbers given in Figure 14 for the UV/vis diffuse reflectance spectra. Light interruptions due to UV/vis measurements are marked with *.

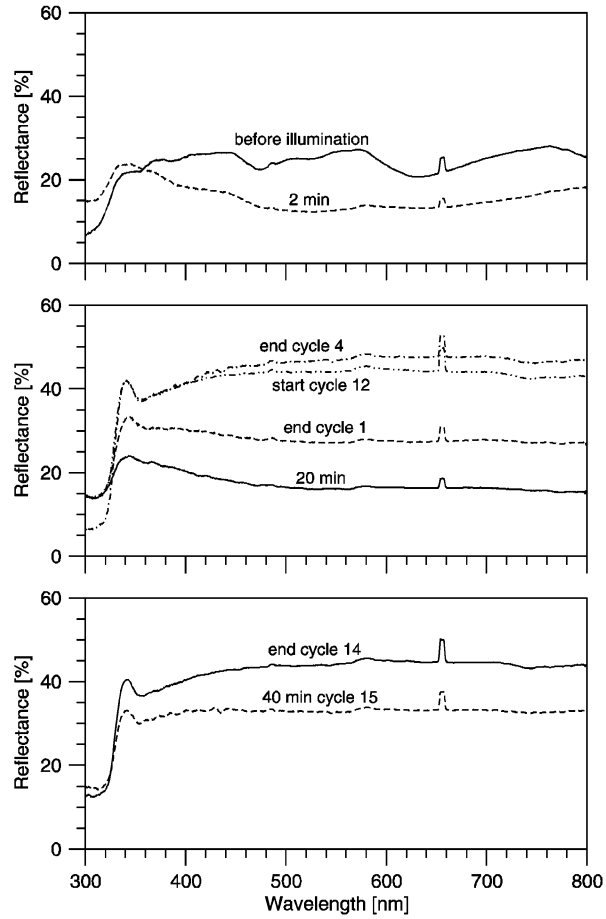

Figure 14. UV/vis diffuse reflectance spectra taken at the indicated times during an experiment with setup 1.

formed on the surface with the more highly reflective layers also having a relatively high surface silver content. This silver, in contrast to the aforementioned species that cause the layer darkening, consists mainly of large particles around 1 μm in size which appear crystalline.[27]

In the lowest part of Figure 14, the upper curve (end cycle 14) shows the reflectance after three cycles without polarization. With the shutter still closed, polarization is resumed, immediately giving rise to a high dark current as the accumulated silver species are reoxidized (see Figure 13). Interestingly, this dark reoxidation does not lead to a noticeable change in layer reflectance. It is not until illumination is resumed along with the polarization that the layer reflectance is significantly affected (see lower curve 40 min cycle 15). The marked decrease in reflectance is likely the result of rapid growth of surface AgCl crystals, which lead to a less reflective morphology.

Conclusions

Silver chloride electrodes photocatalytically oxidize water to O_2 under appropriate conditions. The increased O_2 production of AgCl electrodes which have been prepared by electrochemical oxidation of 50 and 100 nm Ag layers is due to the higher absorptivity of the thicker layer. Addition of bromine during the oxidation process of the Ag-layer resulted in Br-doped AgCl layers that showed higher O_2 production due to higher sensitivity. Further experiments with AgBr-doped AgCl layers will provide a better understanding of the influence of bromide ions on the absorptivity, sensitivity, and reactivity of the photoanode. The results with Br-doped AgCl layers also showed the sensitization approach to be a promising one, and further experiments with other sensitizing species such as Au clusters, Ag_2S, and AgI are challenging. Silver halides can also be prepared by chemical solution deposition.[29] To compare the present results with AgCl layers prepared by this method, further experiments will be carried out.

A thin gold layer on a roughened glass support is sufficient as back contact for the AgCl photoanode. The roughness of the support improves the adhesion and mechanical stability of the layers deposited. With experimental setup 2, AgCl layers on a rough support could be used for several experiments (up to 4), without a strong decrease in photoactivity.

Photoelectrochemical water splitting experiments were carried out with setup 2. The AgCl photoanode was combined with platinum and with semiconductors capable of reducing water to hydrogen upon illumination. The highest O_2 and H_2 production rates in photoelectrochemical water splitting experiments were observed when Pt was combined with AgCl in setup 2. For platinized silicon solar cells, the problematic and difficult electrode preparation, especially the contact to the Au-coated glass support and the fixing with epoxy adhesive, are a drawback. For experiments with p-$GaInP_2$ the comparably low O_2 and H_2 production is due to the small surface of the photocathode. Taking all this into account, the amount of O_2 and H_2 produced can be considered as good and very promising for further experiments. For silicon solar cells or p-$GaInP_2$ as photocathode, the AgCl photoanode still has to be polarized ($\sim$0.65 V vs NHE). Nevertheless, combining these semiconductors with silver chloride makes the overall water splitting photoassisted. It is challenging to work on decreasing the onset potential for both semiconductor photocathodes under illumination by optimizing the platinization process and in the case of silicon solar cells, the contact with the Au-coated supporting glass. This could lead to an overall water splitting system where no external bias has to be applied.

Surface photovoltage spectroscopy provides information for the possible sub-bandgap absorption mechanisms which are an essential feature of this system. For the overall efficiency, the

reflectivity and absorptivity of the surface, which are related to surface morphology play an important role. Certainly, the diffuse reflectance spectra taken alone are very difficult to interpret, given the complex morphological and nonhomogeneous nature of the Ag/AgCl system. The silver species initially formed when the AgCl electrode is illuminated are spectroscopically visible, as seen by the large reflectance decrease, particularly between 380 and 800 nm. The broad band reflectance change indicates that there are likely innumerable different silver species of varying size, from silver clusters to bulk silver which contribute to the spectra. After this point, the morphological change on the layer surface increasingly dominates the spectra and leads to a greater reflectance, the degree of which depends on the amount of bulk silver accumulated on the surface. An efficient reoxidation of silver formed in the photoreaction leads to less reflective and therefore better absorbing electrodes, a reassuring result because the two positive characteristics of photocurrent and absorptivity enhance one another.

Acknowledgment. We acknowledge financial support by the Swiss Federal Office of Energy (project no. 36846) and by the Swiss National Science Foundation (project no. 2000-061259). We thank the workshop staff of the Department of Chemistry and Biochemistry for building the experimental setups, Adrian Schindler for the PVD coating of the glass supports, Beatrice Frey for the SEM images, and René Schraner and Kurt von Escher for their valuable support with all the electronic equipment. We also thank Siemens Solar GmbH (München, Germany) for supplying the silicon solar cells, and the group of Prof. E. Bucher (University of Konstanz, Germany) for cutting them. In addition, we thank J. A. Turner (NREL, Golden, CO) for the p-$GaInP_2$ electrodes.

References and Notes

(1) (a) Special issue of *Biochim. Biophys. Acta Bioenerg.* **2001**, *1503*, 1−259. (b) Zouni, A.; Witt, H. T.; Kern, J.; Fromme, P.; Krauss, N.; Saenger, W.; Orth, P. *Nature* **2001**, *409*, 739.

(2) (a) Ruettinger, W.; Dismukes, G. C. *Chem. Rev.* **1997**, *97*, 1. (b) Yagi, M.; Kaneko, M. *Chem. Rev.* **2001**, *101*, 21. (c) Yagi, M.; Wolf, K. V.; Baesjou, P. J.; Bernasek, S. L.; Dismukes, G. C. *Angew. Chem.* **2001**, *113*, 3009; *Angew. Chem., Int. Ed.* **2001**, *40*, 2925.

(3) Zou, Z.; Ye, J.; Sayama, K.; Arakawa, H. *Nature* **2001**, *414*, 625.

(4) Ishihara, T.; Nishiguchi, H.; Fukamachi, K.; Takita, Y. *J. Phys. Chem. B* **1999**, *103*, 1.

(5) Kato, H.; Kudo, A. *Chem. Phys. Lett.* **1998**, *295*, 487.

(6) Machida, M.; Yabunaka, J.; Kijima, T. *Chem. Mater.* **2000**, *12*, 812.

(7) (a) Sayama, K.; Yoshida, R.; Kusama, H.; Okabe, K.; Abe, Y.; Arakawa, H. *Chem. Phys. Lett.* **1997**, *277*, 387. (b) Wang, H.; Lindgren, T.; He, J.; Hagfeldt, A.; Lindquist, S. E. *J. Phys. Chem. B* **2000**, *104*, 5686.

(8) Khan, S. U. M.; Akikusa, J. *J. Phys. Chem. B* **1999**, *103*, 7184.

(9) Lanz, M.; Schürch, D.; Calzaferri G. *J. Photochem. Photobiol. A: Chem.* **1999**, *120*, 105.

(10) Pfanner, K.; Gfeller, N.; Calzaferri G. *J. Photochem. Photobiol. A: Chem.* **1996**, *95*, 175.

(11) Glaus, S.; Calzaferri, G. *J. Phys. Chem. B* **1999**, *103*, 5622.

(12) Calzaferri, G.; Spahni, W. *J. Photochem.* **1986**, *32*, 151.

(13) James, T. H. *The Theory of the Photographic Process*, 4th ed.; Macmillan: New York, 1977.

(14) Calzaferri, G.; Brühwiler, D.; Glaus, S.; Schürch, D.; Currao, A.; Leiggener, C. *J. Imaging Sci. Technol.* **2001**, *45*, 331.

(15) Glaus, S.; Calzaferri, G.; Hoffmann, R. *Chem. Eur. J.* **2002**, *8*, 1785.

(16) Sumi, S.; Watanabe, T.; Fujishima, A.; Honda, K. *Bull. Chem. Soc. Jpn.* **1980**, *53*, 2742.

(17) (a) Turner, J. A.; Manassen, J.; Nozik, A. J. *Appl. Phys. Lett.* **1980**, *37*, 488. (b) Specht, M.; Kühne, H.-M.; Schefold, J. *Adv. Hydrogen Energy* **1990**, *8*, 815.

(18) Nozik, A. *J. Appl. Phys. Lett.* **1977**, *30*, 567.

(19) (a) Khaselev, O.; Turner, J. A. *Science* **1998**, *280*, 425. (b) Gao, X.; Kocha, S.; Frank, A. J.; Turner, J. A. *Int. J. Hydrogen Energy* **1999**, *24*, 319.

(20) The silicon solar cells where kindly suppiled by Siemens Solar GmbH (München, Germany). They were cut in square pieces of 17 × 17 mm by laser in the group of Prof. E. Bucher (University of Konstanz, Germany).

(21) The p-$GaInP_2$ electrodes were kindly supplied by J. A. Turner (NREL, Golden, CO). (a) Kocha, S. S.; Turner, J. A.; Nozik, A. *J. Electroanal. Chem.* **1994**, *367*, 27. (b) Kocha, S. S.; Turner, J. A. *J. Electrochem. Soc.* **1995**, *142*, 2625.

(22) Memming, R. *Semiconductor Electrochemistry*; Wiley-VCH: Weinheim, 2001.

(23) Vanmaekelbergh, D. Electron Transfer at Electrodes and Interfaces. In *Electron Transfer in Chemistry, Volume 1: Principles, Theories, Methods, and Techniques*; Balzani, V., Ed.; Wiley-VCH: Weinheim, 2001; pp 126−188.

(24) (a) Beer, R.; Binder, F.; Calzaferri, G. *J. Photochem. Photobiol. A: Chem.* **1992**, *69*, 67. (b) Lanz, M.; Calzaferri, G. *J. Photochem. Photobiol. A: Chem.* **1997**, *109*, 87.

(25) Gevantman, L. H. *CRC Handbook of Chemistry and Physics*, 78th ed.; Linde, D. R., Fredrikse, H. P. R., Eds.; CRC Press: Boca Raton, New York, 1998; pp 8-81−8-84.

(26) Kronik, L.; Shapira, Y. *Surf. Sci. Rep.* **1999**, *37*, 1.

(27) Schürch, D. Ph.D. Thesis, University of Bern, Switzerland, 2002.

(28) Marchetti, A. P.; Eachus, R. S. *Adv. Photochem.* **1992**, *17*, 145.

(29) Hodes, G.; Calzaferri, G. *Adv. Funct. Mater.* **2002**, *12*, 501.